An Implicit Algorithm for Finite Volume - Finite Element Coupling

Davor Čokljat¹, Aleksandar Jemcov *2, and Joseph P. Maruszewski³

 $^1\rm ANSYS$ Inc., 6 Europa View, Sheffield, South Yorkshire S9 1XH, UK $^2\rm Aerospace$ and Mechanical Engineering, University of Notre Dame, Notre Dame, IN 46556, USA $^3\rm ANSYS$ Inc., 1007 Church Street Evanston, IL 60201, USA

May 14, 2015

Abstract

We present an implicit coupling algorithm that is suitable for strongly coupled physical problems that were discretized by heterogeneous numerical schemes, namely finite volume and finite element methods. The primary characteristic of the proposed scheme is an implicit treatment of the heterogeneous schemes through a single matrix approach. The finite element and finite volume parts of the discretized domain exchange information through a coupling boundary and the resulting discretization coefficients are stored in a block matrix. The structure of the matrix is such that the coupling coefficients are stored in the off-diagonal blocks of the matrix, while finite element and finite volume subdomains are stored in the diagonal blocks of the matrix. A suite of efficient linear solvers based on the Krylov subspace methods were developed for the solution of the resulting coupling problem. Several demonstration cases that illustrate the coupling algorithm are presented.

Keywords: Finite Element Method (FEM); Finite Volume Method(FVM); Coupling algorithm, Block matrix

Introduction

Multiphysics problems are prevalent in todays engineering practice. It is hard to imagine a device that does not need structural, thermal and fluid flow analysis in order to design it for the safe operation and the peak efficiency. Today's engineering practice rarely undertakes a numerically integrated approach to analyzing and simulating the proposed designs. The current design practice takes an iterative approach to simulations and analysis through a series of the stages that involve the use of computational fluid dynamics, thermal and stress analysis. Numerical difficulties arise in a staged approach due to increased stiffness of the problem and

^{*}Corresponding author ajemcov@nd.edu

the loss of coupling among equations. A typical approach to simulating coupled phenomena involving solids and fluids is done through an exchange of boundary conditions through the coupling boundaries. This process is inherently iterative. The coupling between fields in fluids and solids can be recovered by an iterative procedure in which the fields on the coupling boundaries acting as boundary conditions for different analyses, are updated in this iterative process.

This simulation of coupled problems is further complicated by the use of different simulation practices that involve different discretization methods used for the particular stage of the analysis. In fluid flow, finite volume method is commonly used for the discretization of governing equations. In analyses that involve solid materials finite element is the method of choice for producing the discrete systems of equations. The choice of the discretization method that is being used for a given problem is often dictated by the efficiency and accuracy requirements. The Finite Volume Method (FVM) is often used in computational fluid dynamics (CFD) as a method of choice due to its simplicity and ability to reproduce the conservation laws. The simplicity of the finite volume discretization stems from the fact that the low degree polynomials (C^0) are used for the interpolation within finite volumes. The numerical efficiency of the finite volume schemes stems from the fact that only one integration point per face of the finite volume cell is required to evaluate the numeric flux. This approach yields a low storage numerical scheme that produces very sparse matrices. Furthermore, C^0 interpolation functions used for the representation of the variables within a finite volume cell allows the usage of arbitrary shapes of finite volumes cells, thus simplifying the mesh generation for the domains with the complex geometric shapes. In this work we are concerned with the cell-centered finite volume method that stores all variables in cell centers. Matrix coefficients arising in implicit discretization of the finite volume problems are obtained by evaluating fluxes on the cell face centers. This approach is chosen intentionally given the fact that cell-centered finite volume discretization is the dominant approach in the CFD community. Data structures required for the efficient representation of the finite element connectivity on unstructured meshes of arbitrary shapes is of the so-called face-to-cell type. In practical terms, face-to-cell connectivity allows very fast access to the cell data required for the flux evaluation in the face center.

On the other hand, finite element method is a preferred approach for the problem solution in structural analysis and in computational mechanics in general. Finite element approach to discretization to problems in mechanics offers a strong mathematical foundations that allow for error and convergence estimates even for challenging computational problems. Usage of higher order interpolation polynomials enables a higher order of accuracy when compared to finite volumes for the nominally same size of the computational mesh. The finite element method is particularly well suited for the elliptic problems arising in linear elasticity and structural mechanics. Since the finite element data is stored in the nodes of the finite elements, the data structure required for the representation of the finite element discretization on unstructured meshes consists of node-to-cell connectivity information. Matrix coefficients in the finite element discretization are obtained as the collection of the contributions from all finite elements sharing the particular node.

In recent years researchers have started addressing the problem of coupled sim-

ulations. Geiger at al. [4] proposed an algorithm for coupling of nodal based finite volume and finite elements using overlapping groups of finite elements and finite volumes. Galerikin finite elements were used to provide the second order of accuracy interpolation for flux evaluations on finite volume grid. This approach may be classified as a control volume finite element method using dual grids [1]. Lazarov at al. [5] proposed the method for coupling finite volume-finite elements by using the node based finite volume scheme on dual grids. Sardella [3] proposed a mixed finite element/volume method that used finite volume approach to discretizing convective terms while finite element approach was used for the discretization of the diffusion terms in convection diffusion problems. The mixed algorithm was applied to the singularly perturbed problems in fluid mechanics providing the numerical stability to the computations. Gadeschi at al. [2] proposed the coupling method based on hierarchical Cartesian grids for heat transfer between solids and fluids. Vierndeels [6] and Sicklinger at al. [7] recently proposed frameworks for a general coupling between codes. In both works the idea is based on using the Jacobians of the governing equations to create the coupling conditions for souped simulations. Vierendeels and Sicklinger algorithms are examples of the explicit coupling of black-box solvers within the framework of iterative coupling approach.

It is observed that in the previous attempts to couple finite volume and finite element methods, the approach was to modify one or the other method across the shared interface in order to make the approach more suitable for the discretization. Contrary to that, in this work we maintain the characteristics of each method used for the discretization of the respective part of the domain. Therefore, we propose an approach to coupling that maintains the discretization practices of both finite volume and finite element methods.

A novel implicit coupling algorithm for the mixed discretizations involving finite elements and finite volumes that exchange information along one or more boundaries called coupling interfaces is proposed. The resulting discretization coefficients are stored in a block matrix in which coupling interface coefficients are stored in off-diagonal blocks while the finite element and finite volume discrtizations are stored in diagonal blocks. We propose an algorithm for coupled interfaces that uses native information from each discretization scheme to produce the necessary data for coupling of finite element and finite volume discretizations. The method is conservative and there is no loss of mass, energy or momentum across the interface even though substantially different discretization schemes are used on each side of the interface. Linear solver suite capable of handling block matrices arising in coupled finite element-finite volume discretizations is also developed. Two computational examples are presented as an illustration of the coupled algorithm. The first example demonstrates the coupling of finite elements and finite volumes in the case of the energy equation for the solid with an interface separating finite volume from finite element discretizations. The second example is coupled fluid-solid heat transfer problem in which energy equation is coupled through the solid-to-fluid interface.

Governing equations and boundary conditions

Consider the energy equation in the solid shown in Figure (1)

$$k\partial_i^2 T = f \text{ in } \Omega = \Omega_{FE} \cup \Omega_{FV}.$$
 (1)

Constant heat conduction coefficient independent of spatial location and temperature was assumed. The energy equation is closed by adding the corresponding boundary conditions

$$B(T) = b \text{ on } \Gamma = \Gamma_{FE} \cup \Gamma_{FV}.$$
 (2)

In addition to the solid energy equation, the coupled system might have a fluid domain. In that case, the energy equation in the fluid is given by the convectiondiffusion equation

$$\partial_i(\rho u_i T) = k \partial_i^2 T \text{ in } \Omega = \Omega_{FE} \cup \Omega_{FV},$$
 (3)

supplemented by the boundary conditions

$$C(T) = c \text{ on } \Gamma = \Gamma_{FE} \cup \Gamma_{FV}.$$
 (4)

Equations (1) and (3) represent the steady-state equations of energy transport in solids and fluids. The boundary conditions considered here are of Neumann and Dirichlet type. The computational domain is general is divided in two parts by an internal surface called coupled boundary separating regions where finite volume and finite element discretizations are applied. However, the coupling boundary might be a physical boundary separating fluid from a solid thus representing a physical surface coinciding with the coupling interface.

An internal consistency condition can be added to the governing equations (1) through (4) that enforces the conservation of energy across the coupling interface as illustrated in Figure (1) In simple terms, the energy flux across the coupling interface is preserved and we can write the balance equation

$$\int_{\Gamma^{-}} f_i^- n_i d\Gamma - \int_{\Gamma^{+}} f_i^+ n_i d\Gamma = 0.$$
 (5)

In the case of heat conduction, the consistency condition becomes

$$\int_{\Gamma^{-}} (k\partial_{i}T)_{i}^{-} n_{i} d\Gamma - \int_{\Gamma^{+}} (k\partial_{i}T)_{i}^{+} n_{i} d\Gamma = 0.$$
 (6)

Internal consistency condition is used to produce the consistent interpolations between finite elements and finite volumes for both cases when the interface is an arbitrary surface separating dicretization zones and as well as when the interface coincides with both the physical and discretization boundaries. Consistent interpolation is defined here in terms of the energy conservation as well as in terms of bridging the different requirements for the smoothness of the interpolation functions. In other words, the interface consistency condition must allow conservation of energy even when on one side the data variation within a finite volume cell is represented by functions belonging to C^0 space and o the other side the data variation within a finite volume is represented by C^1 space. We limit our discussion here to interfaces that have C^0 to C^1 (and vice versa) transitions. Higher order transitions are the subject of ongoing research.

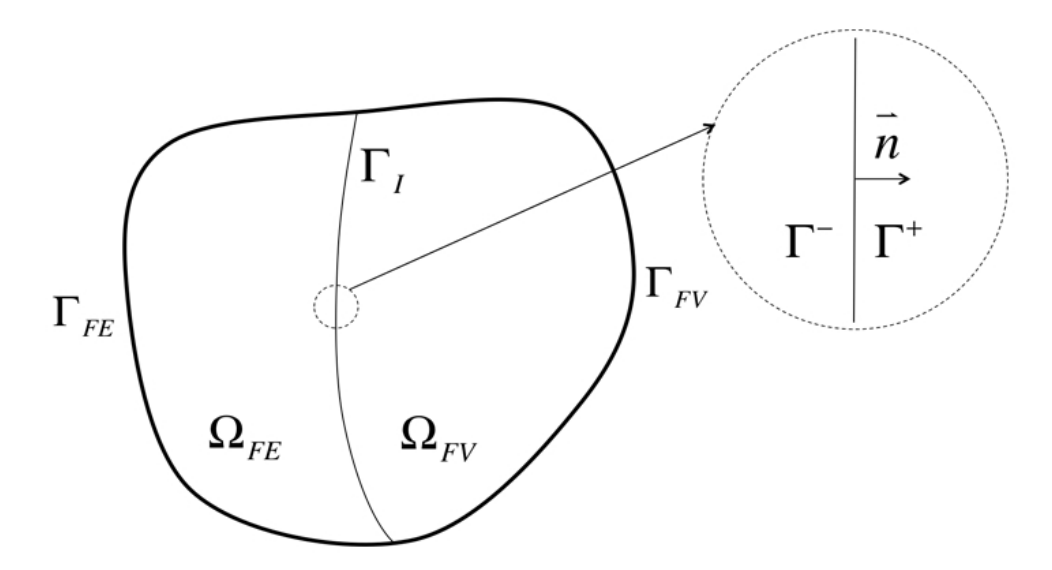


Figure 1: Coupling interface separating either physical domains or arbitrary internal domains discretezed with different numerical schemes

Method of solution

We use two different approaches to discretizing equations (1) and (2), finite volume and finite element methods namely. We consider the computational domain consisting of two parts as depicted in Figure (1). The part denoted by Ω_{FE} together with the boundary Γ_{FE} constitute the domain of the discretization by finite elements. Similarly, the part denoted by Ω_{FV} together with the boundary Γ_{FV} is discretized by the cell-centered finite volume method. Interface Γ_I between two discretization domains is an internal surface that is used to transfer the information between two discretization methods.

Linear 4-node quadratic finite elements with C^1 continuity are used for the finite element basis while the cell centered finite volume discretization with the C^0 interpolation basis is used for the finite volume part of the domain. Finite element and finite volume discretizations are both nominally of the second order of accuracy. In the case of finite elements, the second order of accuracy is achieved by using the shape functions with C^1 continuity. In the case of the finite volume discretization, the second order of accuracy is achieved by evaluating the weak form of the energy equation at the geometric center of the finite volume cell.

Weak form of the energy equation is used for both finite volume and finite element discretizations. The weak form of the energy equation for the solid is obtained by multiplying both sides of Eq. (1) by a test function ξ and integrating over the whole domain Ω

$$\int_{\Omega} k \partial_i^2 T \xi d\Omega = \int_{\Omega} f \xi d\Omega. \tag{7}$$

The cell centered finite volume method is obtained when the test function ξ is chosen to be constant over the finite volume cell and equal to unity i.e., $\xi \in C^0$. In that case Eq (7) in the domain Ω_{FV} is replaced by the conservation law of

energy in the solid

$$\int_{\Gamma_{FV}} k \partial_i T n_i d\Gamma_{FV} = \int_{\Omega_{FV}} f d\Omega_{FV}.$$
 (8)

Vector of local surface normal is denoted by n_i and we used Gauss-Ostrogradsky's theorem to obtain the weak form of the conservation law of energy in the solid.

The finite element method for the case of the energy transport in the solid is obtained through integration by parts Eq. (7)

$$\int_{\Omega_{FE}} k \partial_i T \partial_i \xi d\Omega_{FE} = \int_{\Omega_{FE}} f \xi d\Omega_{FE} + \int_{\Gamma_{FE}} \xi k \partial_i T d\Gamma_{FE}. \tag{9}$$

In this work we use test functions and shape functions that are linear i.e., $\xi \in C^1$.

Standard finite volume and finite element discretizations are obtained when integrals in equations (8) and (9) are replaced by the numerical integration performed in face and cell centers for finite volume and nodes for finite element methods. In addition, partial differentials in Eq. (8) are replaced by finite differences for a given neighboring finite volume cells, leading to the following expression for the surface integral

$$\int_{\Gamma_{FV}} k \partial_i T n_i d\Gamma_{FV} \approx k \frac{T_{c_R} - T_{c_L}}{d} A_{\Gamma_{FV}} + G.$$
 (10)

Symbol d is used to represent the distance between two cell centers while G is the non-orthogonal contribution $A_{\Gamma_{FV}}$ is the surface area of the interface between finite element and finite volume cell. In a general case the direction between two cell centers does not coincide with any of the cartesian directions and the non-orthogonal contribution of the partial derivative, denoted by g_i , has to be added to the expression in Eq. (10). However, here we assume that this contribution was lumped into the right-hand-side of Eq. (8) without any loss of generality. Right hand side of Eq. (8) is evaluated in the cell center of the finite volume cell.

The finite element approximation of Eq. (9) is obtained by assuming that the test and shape functions belong to the same space thus yielding the following expression for the left-hand-side of Eq. (9)

$$k\partial_i T \partial_i \xi = \sum_j k T_{nj} (\partial_i S_j)^2. \tag{11}$$

Symbol S represents a shape function that is in this case chosen to be linear Lagrange polynomial and we have used the linear representation of the temperature field over the finite element $T = \sum_{j} S_{j} T_{nj}$. Right-hand-side of Eq. (9) is evaluated by computing the contributions of each volumetric integral to the nodes of the given finite element.

Standard discretization practices are easily applied throughout respective discretization domains. However, in order to complete the discretization of the whole domain $\Omega = \Omega_{FE} \cup \Omega_{FV}$ the question of the discretization along the interface Γ_I must be addressed.

Figure (2) depicts a dEtail the interface Γ_I where we can see finite element being a neighbor to a finite volume cell connected but the common face Γ_I^e . We use the consistency condition in Eq. (5) to complete the discretization for finite element-finite volume couple. The consistency condition states that the in order to conserve the energy in the domain then the energy flux leaving one domain

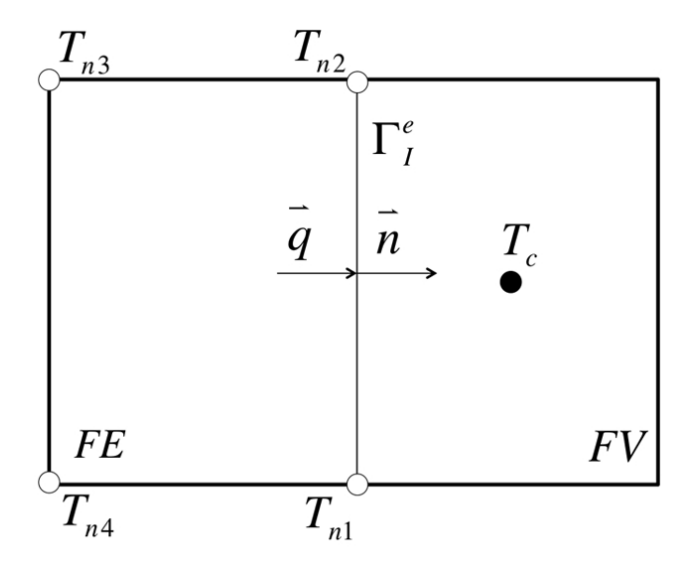


Figure 2: Finite element-finite volume pair sharing a common face that is a part of the Γ_I interface. Black circle represents the finite volume cell center while open circles represent the nodes of finite element.

along the interface Γ_I must be equal to the energy entering the other domain across the same interface Γ_I . Therefore, in order to complete the discretization along the Γ_I interface we must find the expression for the flux across across every face connecting finite elements and finite volumes Γ_I^e .

This expression is obtained by approximating the flux across the interface by the finite difference between finite volume and finite element centroid values

$$\int_{\Gamma_I^e} k \partial_i T n_i d\Gamma_I^e \approx k_f \frac{T_c - \sum S_i(T_{ni})_c}{d} A_{\Gamma_I^e} + G.$$
 (12)

Expression $\sum (S_i T_{ni})_c$ is the finite element interpolation of the temperature field in the centroid of the finite element, T_c is the value of the temperature field at the finite volume centroid, $A_{\Gamma_I^e}$ is the surface area between finite volume and finite element and G is the non-orthogonal contribution due to misalignment of the face normal and the direction defined by the cell distance. Since Eq. (5) requires that the fluxes on both sides of the interface Γ_I are equal, Eq. (12) is used to complete the discretization on along the interface. It should be noted that the same expression Eq. (12) is used to compute the coupling matrix entries for both finite element and finite volume discretizations. The resulting matrix structure is shown in Figure (3).

The off-diagonal entries in the block matrix $A_{\Gamma_{C^1}^{C^0}}$ and $A_{\Gamma_{C^0}^{C^1}}$ are obtained by computing the contributions to the finite element and finite volume system of equations using Eq. (12). The consistency condition given by Eq. (5) produces the contributions to finite element and finite volume side of the interface so that the finite volume side (Γ^+) has the following entries:

$$A_{FV} = \left[k_f \frac{T_c}{d} A_{\Gamma_I^e} \right]^-, \tag{13}$$

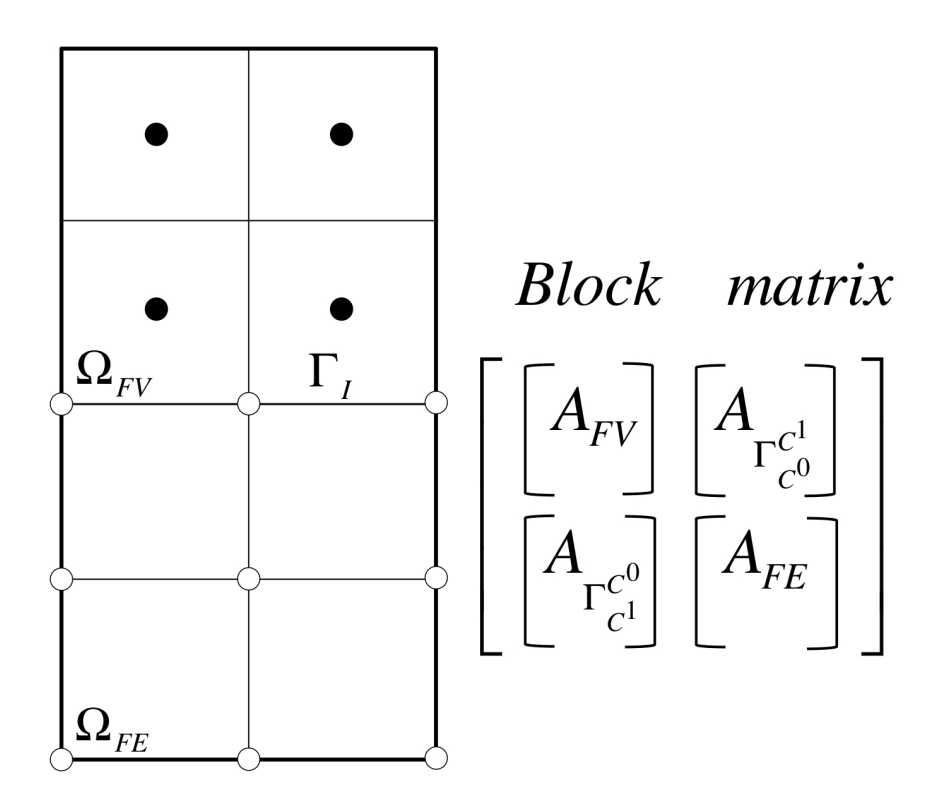


Figure 3: Matrix structure for the coupled finite element-finite volume discretization.

$$A_{\Gamma_{C^0}^{C^1}} = \left[-k_f \frac{(\sum S_i T_{ni})_c}{d} A_{\Gamma_I^e} \right]^-. \tag{14}$$

The symbol k_f is the surface heat conduction coefficient evaluated by using the harmonic averaging procedure. It should be noted that the expression in Eq. (13) is the contribution to the the block matrix A_{FV} at the interface while Eq. (14) is the contribution to the coupling block matrix $A_{\Gamma_{c1}^{0}}$. The non-orthogonal contribution G is added to the right hand side of the finite volume block. Similarly, finite element discretization produces the following contributions:

$$A_{FE} = \left[-\frac{k_f}{2} \frac{(\sum S_i T_{ni})_c}{d} A_{\Gamma_I^e} \right]^+, \tag{15}$$

$$A_{\Gamma_{C^1}^{C^0}} = \left[\frac{k_f}{2} \frac{T_c}{d} A_{\Gamma_I^e} \right]^+. \tag{16}$$

The finite element discretization of the element produces the contribution to the diagonal block matrix A_{FE} as well as to the off-diagonal coupling block $A_{\Gamma_{C_0}^{C_1}}$. Since the consistency condition specifies the flux for the finite element face of the interface Γ_I^e , the nodes that reside on the interface receive the half of the flux due to linear interpolation as indicated in Eq. (15) and (16). The non-orthogonal correction is is similarly interpolated and added as the contribution to the coefficients $A_{\Gamma_{C_0}^{C_1}}$.

Eq. (12) implicitly uses the fact that the flux across the face Γ_I^e is evaluated using the pointwise values of the temperature field instead of cell averages. This transition between pointwise and cell averages is possible due to the fact that the pointwise values coincide with the cell averages if the function is evaluate at the cell centroid for the finite volumes of second order of accuracy. Therefore, even though the test functions for finite element and finite volume methods belong to different spaces of continuous functions, the transition from C^1 to C^0 functions is enabled throughout the use of pointwise values in finite volume method thus matching the desired interpolation continuity requirements. Clearly, the higher order transition, for example C^2 to C^0 will require the reconstruction of the pointwise values in the finite volume domain that will recover the desired continuity requirements. This is the subject of the ongoing research work.

Once the off-diagonal coupling coefficient have been computed, the diagonal entries in the block matrix A_{FV} and A_{FE} are obtained by applying the standard discretization practices applicable to finite volume and finite element discretization schemes. The resulting system represents a fully coupled system that is solved by the linear algebra suite. Each block in the coupled matrix A is represented through a sparse matrix structure utilizing the compressed-row format to save the memory. However, it should be noted that the implementation of the linear algebra library allows for storage of dense blocks as well. The linear algebra library implements Krylov subspace algorithms including conjugate gradient (CG), biconjugate gradient stabilized (BCGSTB), transpose free qausi-minimum residual (TFQMR). In addition, algebraic multigrid solver (AMG) based on aggregation of neighbors has been implemented to operate on the coupled block matrix. Consistent restriction and prolongation operators have been implemented so that the block matrix can be consistently defined on the progression of coarse levels.

Results and discussions

In this section we present the results for the two cases of the coupled systems. The first case is represented by the energy transport in the solid with the boundary conditions as depicted in Fig. (4). The upper half of the domain was discretizated by the cell-centered finite volume method while the lower half of the domain was discretizated by the linear quadratic finite elements. Since there is no jump in material properties and given the adiabatic conditions on the sides, the solution to this problem is a linear variation of the temperature between 300 K and 400 K in the vertical direction. The mesh is fully orthogonal and there was no non-orthogonal contribution in the discretizated system of equations. The computed temperature profiles at two locations are shown in Fig. (5) and (6). The agreement between analytical and the b=numerical solution if excellent as the analytical behavior of the temperature is recovered. It should be observed that the temperature was plotted at the nodes of the finite element plot in Fig. (5). For the finite volume portion of the domain the temperature was plotted in the cell centers as shown in (6). This explains the offset of the plot in the x-direction.

The second case considered in this work is the coupled energy transport between fluid and solid domains as depicted in Fig. (7). Boundary conditions are given in Fig. (7). The fluid portion of the domain was discretized with the cellcentered finite volume schemes while the solid part was discretized using the linear quadratic finite elements. Since the problem involves the fluid flow, the boundary layer formed at the surface of the solid wall is largely responsible for the heat transfer to and from the fluid. For the given inlet velocity and length of the domain, the Reynolds number based on the length is very low Re = 400, well below the transitional Reynolds number for the flat plate (500,000). Therefore, the flow over the surface of the solid is laminar. The computed temperature profiles and the comparison to the theoretical one is given in Fig. (8) and (9).

Conclusion

We introduced a novel algorithm for finite element-finite volume coupling that is based on the native cell-centered finite volume and linear quadratic finite element discretization methods in their respective parts of the computational domain. The coupling coefficients required for the implicit representation of the coupled matrix were defined. The consistency condition that is based on the flux conservation between finite element and finite volume discretizaitons was defined and used to define the coupling coefficients. Block matrix linear solver based on BCGSTAB was used to solve the coupled solver in one matrix thus producing the implicitly coupled solution. Two examples of the application of the newly defined coupled method were provided. The first example was the energy transport in the solid body discretized in part by finite volume and the other part by finite element technique. The solution was compared to the analytical solution and the excellent agreement was achieved. The second case that was considered consisted of the energy transport between fluid and solid domains. The fluid domain was discretized but the cell-centered finite volume while the solid part was discretized by the linear quadratic finite element scheme. The agreement between analytical and numerical solution, in all cases, is very good.

References

- [1] B.R. Baliga and S.V. Patankar. A new finite-element formulation for convection diffusion problems. *Numerical Heat Transfer*, 3:393–409, 1980.
- [2] B. Gadeschi L. Schneiders M. Meinke and W. Schroeder. A numerical method for multi physics simulations based on hierarchical cartesian grids. *Journal of Fluid Science and Technology*, 10, 2015.
- [3] M. Sardella. On a coupled finite element-finite volume method for convection diffusion problems. *IMA Journal of Numerical Analysis*, 20:281–301, 2000.
- [4] S. Geiger S. Roberts S.K. Matthai C. Soppou and A. Burri. Combining finite element and finite volume methods for efficient multiphase flow simulations in highly heterogeneous ans structurally complex geologic media. *Geofluids*, 44:284–299, 2004.
- [5] R.D. Lazarov J.E. Pasciak P.S. Vassilevsk. Coupling mixed and finite volume discretizations of convection-diffusion-reaction equations on non-matching grids. Symposium on Finite Volume Methods for Complex Applications, 1999.

$ICCM2015, 14-17^{th} July, Auckland, NZ$

- [6] J. Vierendeels. Strong coupling of partitoined fluid-structure interaction problems with reduced order models. European Conference on Computational Fluid Dynamics, ECCOMAS CFD 2006, 2006.
- [7] S. Sicklinger V. Belsky B. Engelmann H. Elmqvist H. Olsson R. Wuchner and K.-U. Bletzinger. Interface jacobian-based co-simulation. *International Journal for Numerical Methods in Engineering*, 98:418–444, 2014.

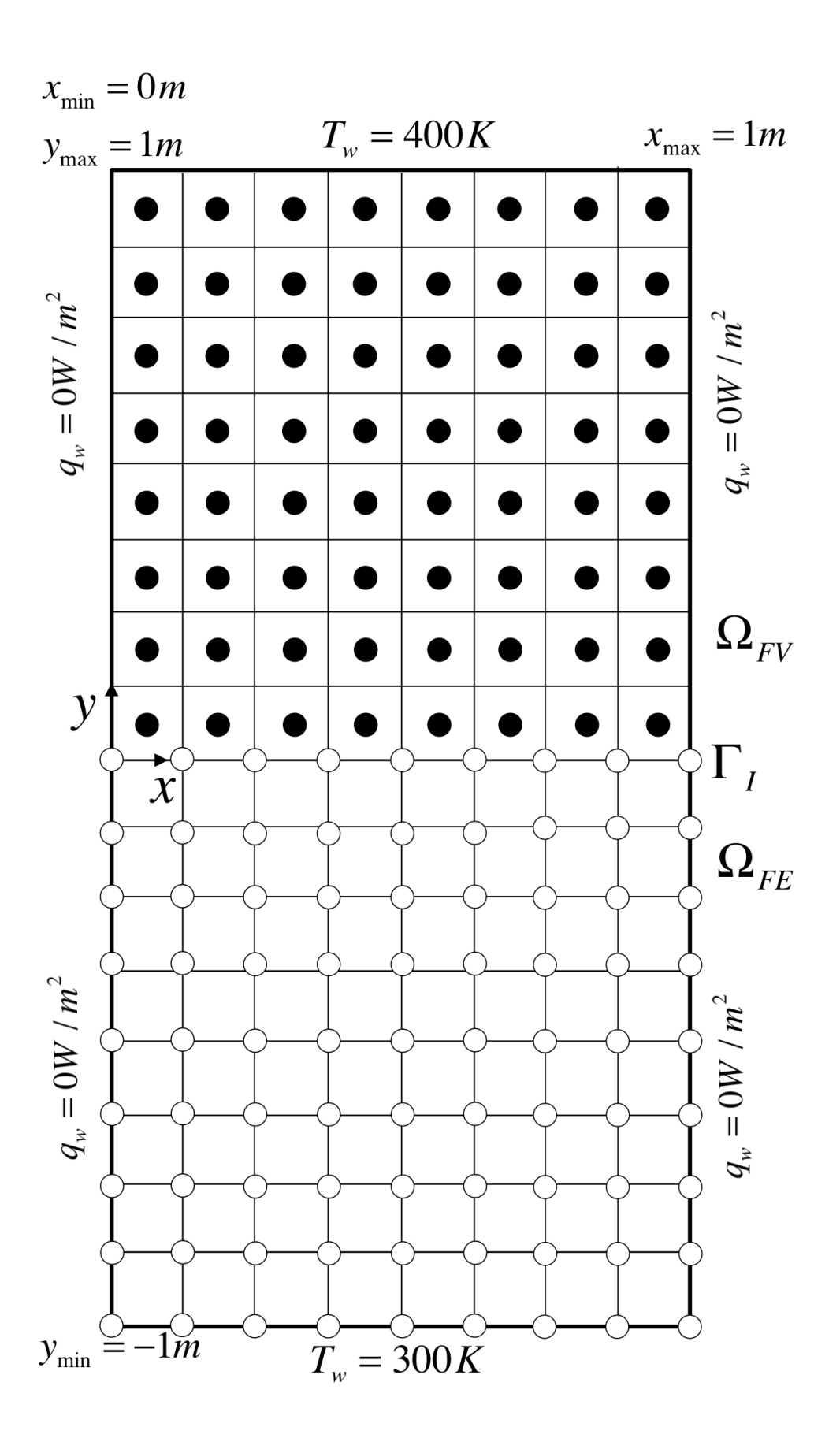


Figure 4: Computational domain for energy transport in a solid.

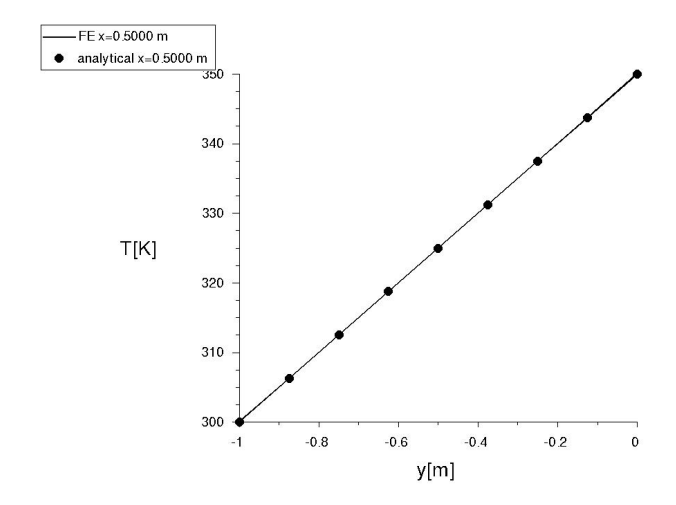


Figure 5: Temperature profile in the vertical direction for the case of the energy transport in the solid for the finite element portion of the domain at the location x = 0.5 m. Solid line represents the numerical whereas dots represent the analytical solution.

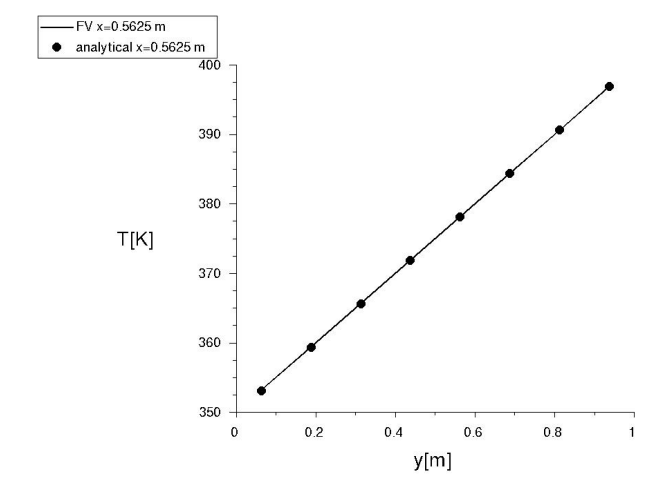


Figure 6: Temperature profile in the vertical direction for the case of the energy transport in the solid for the finite volume portion of the domain at the location $x = 0.625 \, m$. Solid line represents the numerical whereas dots represent the analytical solution.

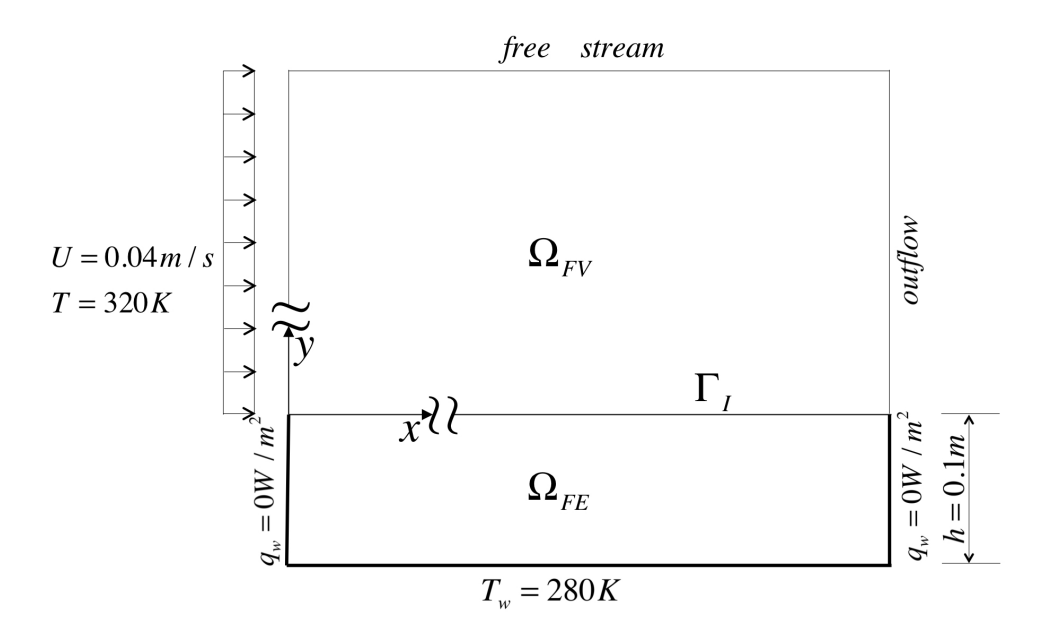


Figure 7: Computational domain for the fluid-solid energy transport.

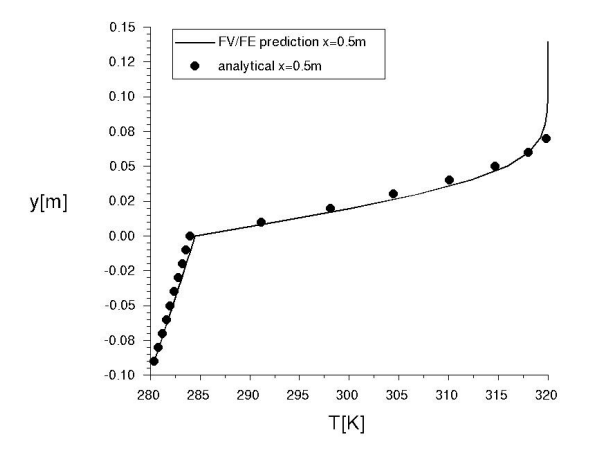


Figure 8: Temperature profile in the vertical direction for the case of the energy transport in the fluid-solid system for the finite element portion of the domain at the location $x = 0.5 \, m$. Solid line represents the numerical whereas dots represent the analytical solution.

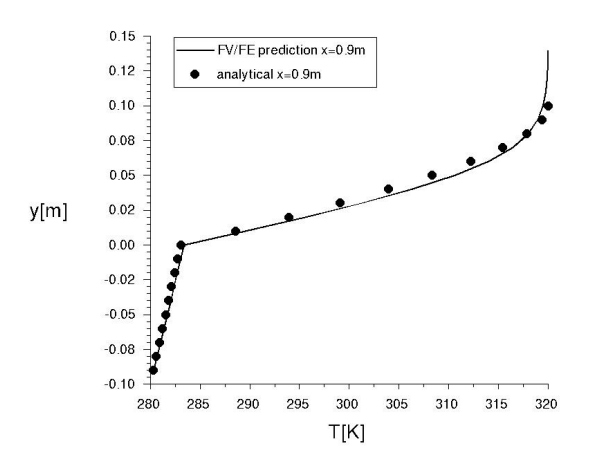


Figure 9: Temperature profile in the vertical direction for the case of the energy transport in the solid for the finite volume portion of the domain at the location $x=0.625\,m$. Solid line represents the numerical whereas dots represent the analytical solution.